Monthly Notices
of the
ROYAL ASTRONOMICAL SOCIETY

MNRAS **447,** 117–131 (2015) doi:10.1093/mnras/stu2384

Interacting supernovae and supernova impostors. SN 2007sv: the major eruption of a massive star in UGC 5979

L. Tartaglia,[1,2★] A. Pastorello,[2] S. Taubenberger,[3] E. Cappellaro,[1] J. R. Maund,[4] S. Benetti,[1] T. Boles,[5] F. Bufano,[6] G. Duszanowicz,[7] N. Elias-Rosa,[1,8] A. Harutyunyan,[9] L. Hermansson,[10] P. Höflich,[11] K. Maguire,[12] H. Navasardyan,[1] S. J. Smartt,[4] F. Taddia[13] and M. Turatto[1]

[1]*INAF-Osservatorio Astronomico di Padova, Vicolo dell'Osservatorio 5, I-35122 Padova, Italy*
[2]*Dipartimento di Fisica e Astronomia, Universitá degli Studi di Padova, Vicolo dell'Osservatorio 2, I-35122 Padova, Italy*
[3]*Max-Planck-Institut für Astrophysik, Karl-Schwarzschild-Str. 1, D-85748 Garching, Germany*
[4]*Astrophysics Research Centre, School of Mathematics and Physics, Queen's University Belfast, Belfast BT7 1NN, UK*
[5]*Coddenham Astronomical Observatory, Suffolk IP6 9QY, UK*
[6]*Departamento Ciencias Fisicas, Universidad Andrés Bello, Avda. Republica 252, Santiago de Chile 8320000, Chile*
[7]*Moonbase Observatory, Otto Bondes vag 43, SE-18462 Akersberga, Sweden*
[8]*Institut de Ciències de l'Espai (CSIC - IEEC), Facultat de Ciències, Campus UAB, E-08193 Bellaterra, Spain*
[9]*Fundación Galileo Galilei - INAF, Telescopio Nazionale Galileo, Rambla JoséAnaFernández Pérez 7, E-38712 Breña Baja, Tenerife, Spain*
[10]*Sandvretens Observatory, Linnégatan 5A, SE-75332 Uppsala, Sweden*
[11]*Department of Physics, Florida State University, 315 Keen Building, Tallahassee, FL 32306-4350, USA*
[12]*European Southern Observatory (ESO), Karl Schwarschild Strasse 2, D-85748 Garching bei München, Germany*
[13]*The Oskar Klein Centre, Department of Astronomy, Stockholm University, AlbaNova, SE-10691 Stockholm, Sweden*

Accepted 2014 November 10. Received 2014 November 10; in original form 2014 March 24

ABSTRACT

We report the results of the photometric and spectroscopic monitoring campaign of the transient SN 2007sv. The observables are similar to those of Type IIn supernovae, a well-known class of objects whose ejecta interact with pre-existing circumstellar material (CSM). The spectra show a blue continuum at early phases and prominent Balmer lines in emission; however, the absolute magnitude at the discovery of SN 2007sv ($M_R = -14.25 \pm 0.38$) indicate it to be most likely a supernova impostor. This classification is also supported by the lack of evidence in the spectra of very high velocity material as expected in supernova ejecta. In addition, we find no unequivocal evidence of broad lines of α- and/or Fe-peak elements. The comparison with the absolute light curves of other interacting objects (including Type IIn supernovae) highlights the overall similarity with the prototypical impostor SN 1997bs. This supports our claim that SN 2007sv was not a genuine supernova, and was instead a supernova impostor, most likely similar to the major eruption of a luminous blue variable.

Key words: supernovae: individual: SN 2007sv – galaxies: individual: UGC 5979.

1 INTRODUCTION

With the label of *supernova* (SN) *impostors,* we refer to a class of objects showing luminous outbursts that mimic the behaviour of real SNe (see e.g. Van Dyk et al. 2000; Maund et al. 2006; Van Dyk & Matheson 2012; Dessart et al. 2009). The most classical SN impostors are thought to be the eruptions of extragalactic luminous blue variables (LBVs; Humphreys & Davidson 1994). They may experience eruptions with comparable energies as those of real SNe, but the stars survive the eruptive events.

LBVs are evolved, massive stars very close to the classical Eddington limit, showing irregular outbursts and, occasionally, even giant eruptions during which they lose massive portions of their H-rich envelope (up to a few solar masses per episode). In quiescence they are blue stars located in the so-called S Doradus Instability Strip of the HR diagram, namely in the luminosity-temperature range $-9 \leq M_{\rm bol} \leq -11$ and 14 000 K $\leq T_{\rm eff} \leq$ 35 000 K (Wolf 1989). During eruptive episodes LBVs become redder and evolve with a roughly constant bolometric magnitude. However, it has been

★ E-mail: leonardo.tartaglia@oapd.inaf.it

proposed that they may increase their bolometric luminosity during giant eruptions (Humphreys & Davidson 1994). Active LBVs show quite erratic variability and, sometimes, fast optical luminosity declines after the outburst, possibly because of prompt dust formation in the circumstellar environment. Spectroscopic studies indicate that eruptions are accompanied with relatively high-velocity winds, viz. a few hundred km s^{-1}. Their spectra share some similarity with those of Type IIn SNe, with prominent and narrow hydrogen lines in emission (Van Dyk et al. 2000).

SN impostors are believed to be extra-Galactic counterparts of the famous 'Giant Eruption' of the Galactic LBV η Carinae in the mid-19th century. This, together with the eruption of P Cygni in the 17th century, are the only two major eruptions registered in the Milky Way in recent times. However, weaker eruptions were occasionally observed in the past either in the Milky Way (e.g. AG Car) or in the Local Group (e.g. S Doradus in the Large Magellanic Cloud; Humphreys & Davidson 1994). These nearby examples are fundamental to our understanding of the nature of eruptive phenomena since their physical parameters are well constrained, and give us the opportunity to demonstrate that these stars survive major eruptions.

It has been argued that a connection may exist between interacting SNe and impostors, mainly based on the observed similarity in the spectra, although they usually have remarkably different photometric properties. Even more importantly, there is evidence (though debated) that LBVs or other massive stars may explode as real interacting SNe soon after major outbursts (e.g. Pastorello et al. 2007; Mauerhan et al. 2013; Ofek et al. 2013; Margutti et al. 2014; Smith, Mauerhan & Prieto 2014) or, at least, that interacting SNe are connected with massive stars compatible with LBVs (Kotak & Vink 2006; Gal-Yam & Leonard 2009, and references therein).

In this context, we report the case of SN 2007sv. The transient was discovered on 2007 December 20.912 UT, and was located 6.9 arcsec west and 6.7 arcsec south of the centre of UGC 5979 (Duszanowicz, Boles & Corelli 2007). The detection was confirmed with an unfiltered CCD image by TB on 2007 December 25.971 UT, whilst there was no source detected at the position of SN 2007sv on an archive image taken on 2007 September 13.093 UT (Duszanowicz et al. 2007).

This article is organized as follows. In Section 2, we report comprehensive information about the host galaxy and in Sections 3 and 4, we present the results of our photometric and spectroscopic observations, respectively. A discussion follows in Section 5, where we remark similarities and differences between 2007sv and other interacting events. Finally, our main conclusions are summarized in Section 6.

Hereafter, we will refer to SN impostors reporting their names without the 'SN' prefix, in order to emphasize their different nature compared to genuine SNe.

2 THE HOST GALAXY

The host galaxy, UGC 5979, is a low-contrast faint (with apparent *B* magnitude 15.93) dwarf galaxy without a visible nucleus. Dwarf galaxies are the most common galaxies in the Universe. Grebel (2001) considers all galaxies with absolute magnitude fainter than $M_V \simeq -18$ as dwarfs, while according to Tammann (1994) the limit usually is $M_B \simeq -16$. According to their optical appearance they are classified into five different groups: dwarf irregulars (dIs), blue compact dwarfs (BCDs), dwarf ellipticals (dEs), dwarf spheroidals (dSphs) and dwarf spirals (dSs). However, this morphological classification is somewhat arbitrary, and the distinction between different classes is sometimes ambiguous.[1]

UGC 5979 is a diffuse (dI) galaxy,[2] (Paturel et al. 2003) located at RA = 10:52:41.16 and Dec = +67:59:18.8 [J2000], with a radial velocity corrected for the Local Group infall on to the Virgo cluster of about 1376 km s^{-1} ($z = 0.0045$). From the above value of the recessional velocity, we infer a distance for UGC 5979 of about 18.85 ± 1.03 Mpc, resulting in an absolute magnitude of $M_B = -15.5$ (distance modulus $\mu \simeq 31.38 \pm 0.27$ mag, adopting $H_0 = 73$ km s^{-1} Mpc^{-1}).

For the foreground Galactic extinction, we assumed the value $A_V = 0.048$ mag, as derived from the Schlafly & Finkbeiner (2011) recalibration of the Schlegel, Finkbeiner & Davis (1998) infrared-based dust maps available e.g. in NED.[3] We also adopt no additional host galaxy extinction contribution in the transient direction, since a detailed analysis of the spectra of 2007sv revealed no evidence of narrow absorptions of the Na ID doublet at the recessional velocity of the host galaxy.

A rough estimate of the metallicity of the host galaxy can be obtained from the relation of Pilyugin, Vílchez & Contini (2004):

$$12 + \log(\mathrm{O/H}) = 5.80(\pm 0.017) - 0.139(\pm 0.011) M_B, \quad (1)$$

that links the integrated absolute *B*-band magnitude with the average oxygen abundance of the galaxy, providing a value of ∼8, which suggests that the environment may have a significantly sub-solar metallicity. A direct measurement of the host galaxy metallicity confirms this result. We spectroscopically observed UGC 5979 with the Nordical Optical Telescope (NOT) equipped with ALFOSC+grism#4. A 1.0 arcsec slit was placed on a bright H II region at 19.5 arcsec (1.8 kpc) from SN 2007sv. After 1800 s exposure, we obtained an optical spectrum with clear detection of narrow [O III] λ5007 Å, [O III] λ4959 Å, Balmer lines up to Hγ, [N II] λ6584 Å and [S II]. Via Balmer decrement, we determined an extinction of $E(B - V) = 0.82$ mag at the H II region location and we corrected the spectrum accordingly. We measured the line fluxes by fitting them with Gaussians, as explained in detail in Taddia et al. (2013). The detection of N II, Hα, Hβ and O III lines allowed us to determine the oxygen abundance via strong line diagnostics, namely with the N2 and O3N2 methods (Pettini & Pagel 2004). Our results are log(O/H)+12 (N2) = 8.01–8.1 dex and log(O/H)+12 (O3N2) = 8.00–8.08 dex. The quoted uncertainty is due to the error on the flux of N II, which appears rather faint. Sub-solar metallicities may be a rather common characteristic of SN impostor environments (see Habergham et al. 2014) and we are currently investigating this issue for a large sample of impostor environments (Taddia et al., in preparation).

3 PHOTOMETRY

3.1 Data reduction and light curves

Our photometric monitoring campaign started on 2007 December 30 and spanned a period of about 100 d. We also collected sparse observations (mostly unfiltered) from amateur astronomers.

[1] Further sub-classification is based on the revised de Vaucouleurs morphological classification introduced by van den Bergh (1960) and on the luminosity classification introduced by van den Bergh (1960, and extended by Corwin, de Vaucouleurs & de Vaucouleurs 1985).
[2] http://leda.univ-lyon1.fr/
[3] http://ned.ipac.caltech.edu

Table 1. Optical magnitudes of 2007sv and associated errors.

Date	MJD	*U*	err	*B*	err	*V*	err	*R*	err	*I*	err	Instrument
20070913	54356.09	–	–	–	–	–	–	>18.8	–	–	–	SX MX7
20071220	54454.91	–	–	–	–	–	–	17.161	0.261	–	–	SX MX7
20071227	54461.86	–	–	–	–	17.975	0.356	17.502	0.137	–	–	MX916
20071230	54464.15	–	–	18.502	0.077	18.161	0.039	17.786	0.023	17.432	0.023	AFOSC
20080104	54469.04	19.145	0.147	18.860	0.025	18.220	0.014	17.812	0.024	–	–	RATCam
20080106	54471.08	19.211	0.057	18.914	0.042	18.271	0.017	17.877	0.018	17.350	0.020	RATCam
20080108	54473.21	19.264	0.085	18.963	0.025	18.225	0.019	17.802	0.029	17.327	0.020	RATCam
20080110	54475.14	–	–	19.044	0.066	18.219	0.027	17.863	0.028	17.329	0.026	AFOSC
20080110	54475.20	19.348	0.076	19.064	0.024	18.252	0.015	17.776	0.030	17.338	0.017	RATCam
20080112	54477.25	19.373	0.025	19.124	0.024	18.311	0.026	17.929	0.033	17.522	0.032	ALFOSC
20080113	54478.00	19.420	0.081	19.166	0.027	18.319	0.016	17.832	0.032	17.382	0.035	RATCam
20080116	54481.12	19.544	0.138	19.208	0.020	18.354	0.026	17.768	0.029	17.452	0.028	RATCam
20080118	54483.20	19.933	0.213	19.392	0.102	18.359	0.034	17.951	0.127	–	–	RATCam
20080120	54485.94	–	–	–	–	–	–	17.984	0.265	–	–	SX MX7
20080128	54493.16	–	–	19.512	0.109	18.573	0.030	18.020	0.068	17.467	0.085	CAFOS
20080128	54493.95	–	–	19.526	0.037	18.520	0.022	17.907	0.023	17.406	0.024	RATCam
20080207	54503.93	–	–	19.885	0.036	18.696	0.021	18.030	0.025	17.514	0.032	RATCam
20080209	54505.94	–	–	–	–	–	–	18.023	0.179	–	–	Apogee Ap7
20080211	54507.85	–	–	–	–	–	–	18.178	0.210	–	–	SBIG ST-7
20080213	54509.94	–	–	–	–	–	–	18.166	0.218	–	–	SX MX7
20080301	54526.88	–	–	20.532	0.053	19.211	0.028	18.328	0.041	17.843	0.056	RATCam
20080304	54529.01	–	–	–	–	–	–	18.599	0.262	–	–	SX MX7
20080305	54530.98	–	–	>20.4	–	19.471	0.056	18.456	0.067	17.854	0.035	CAFOS
20080331	54556.00	–	–	>21.2	–	20.803	0.057	19.455	0.064	18.936	0.049	ALFOSC
20080401	54557.93	–	–	>21.4	–	21.074	0.047	19.745	0.044	19.177	0.184	RATCam

Notes. The observations were carried out using the 2.56 m NOT with ALFOSC and the 2 m Liverpool Telescope with RATCam (both located at the Roque de Los Muchachos, La Palma, Canary Islands, Spain), the Calar Alto 2.2 m Telescope with CAFOS (Sierra de Los Filabres, Spain) and the 1.82 m Copernico Telescope with AFOSC (Mount Ekar, Asiago, Italy). Additional observations (mostly unfiltered) were obtained by amateur astronomers.
The magnitudes obtained from SX MX7, Apogee Ap7 and SBIG ST-7 were computed from unfiltered images, whose magnitudes were rescaled to the *R* band.
MX916: 0.45 m f4.5 Newtonian telescope with an MX916 CCD Camera, at Mandi Observatory (Pagnacco, Udine, Italy)
SX MX7: 0.32 m f/3.1 reflector and a Starlight Xpress MX716 CCD camera at Moonbase Observatory (Akersberga, Sweden)
Apogee AP7: C-14 Celestron Schmidt Cassegrain reflector and an Apogee AP7 CCD camera (Suffolk, United Kingdom)
SBIG ST-7: 0.44 m f4.43 telescope with an SBIG ST-7 Dual CCD Camera at Sandvretens Observatorium (Uppsala, Sweden).

Information about the photometric data and the instruments used are reported in Table 1.

All data were pre-processed using standard procedures in IRAF[4] including bias and flat-field corrections. To measure the magnitudes we used a dedicated pipeline developed by one of us (EC), that consists of a collection of PYTHON scripts calling standard IRAF tasks (through PYRAF) and other specific analysis tools, in particular SEXTRACTOR for source extraction and star/galaxy separation, DAOPHOT to measure the source magnitude via point spread function (PSF) fitting and HOTPANTS[5] for image difference with PSF match.

The magnitudes were measured using the PSF-fitting technique, first subtracting the sky background calculated using a low-order polynomial fit (typically a second-order polynomial). The PSF was obtained by averaging the profiles of isolated field stars. The fitted source is removed from the original frames, then a new estimate of the local background is derived and the fitting procedure is iterated. Finally, the residuals are visually inspected to validate the fit.

Error estimates were obtained through artificial star experiments in which a fake star, of magnitude similar to that of the SN, is placed in the PSF-fit residual image in a position close to, but not coincident with that of the real source. The simulated image is processed through the PSF-fitting procedure and the dispersion of measurements out of a number of experiments (with the fake star in slightly different positions), is taken as an estimate of the instrumental magnitude error. This is combined (in quadrature) with the PSF-fit error returned by DAOPHOT.

The SN photometry was calibrated as follows. Among the observational data, we selected the frames obtained in photometric nights in which standard photometric fields (from the list of Landolt 1992) were observed. These standard frames were used to derive zero-points and colour terms for the specific instrumental set-up and to calibrate the magnitudes of selected stars in the SN field (Table 2 and Fig. 1). This local sequence was used to calibrate the SN magnitudes in non-photometric nights. The final magnitudes were computed using first-order colour-term corrections.

The resulting magnitudes of 2007sv are reported in Table 1 along with the photometric errors, and the light curves are shown in Fig. 2.

3.2 Constraining the SN age

Since no observation was obtained a short time before the discovery of 2007sv, the epochs of the outburst on-set and the light-curve maximum cannot be precisely constrained. None the less, we have adopted the epoch of the discovery as reference time for the light-curve phases, assuming that the transient was discovered in the

[4] IRAF is distributed by the National Optical Astronomy Observatory, which is operated by the Associated Universities for Research in Astronomy, Inc., under cooperative agreement with the National Science Foundation.
[5] http://www.astro.washington.edu/users/becker/hotpants.html

Table 2. Magnitudes of the stellar sequence used for the photometric calibration. The stars are shown in Fig. 1.

Label	RA [J2000] (hh:mm:ss)	Dec [J2000] (dd:mm:ss)	*U*	err	*B*	err	*V*	err	*R*	err	*I*	err
1	10:53:02.62	67:58:18.77	–	–	–	–	20.159	0.056	19.202	0.015	–	–
2	10:53:01.92	67:59:46.33	18.451	0.020	17.110	0.015	15.861	0.029	14.983	0.022	14.214	0.027
3	10:52:54.29	67:58:14.49	15.692	0.009	15.675	0.007	15.127	0.020	14.800	0.016	14.429	0.030
4	10:52:50.03	67:57:21.82	–	–	20.571	0.010	19.113	0.024	18.195	0.015	16.425	0.014
5	10:52:49.13	67:58:39.87	17.682	0.007	17.088	0.011	16.212	0.012	15.688	0.008	15.180	0.012
6	10:52:43.00	67:57:22.46	16.401	0.004	16.329	0.005	15.661	0.010	15.295	0.006	14.887	0.003
7	10:52:27.18	68:00:26.52	–	–	–	–	18.245	0.013	17.770	0.005	17.299	0.015

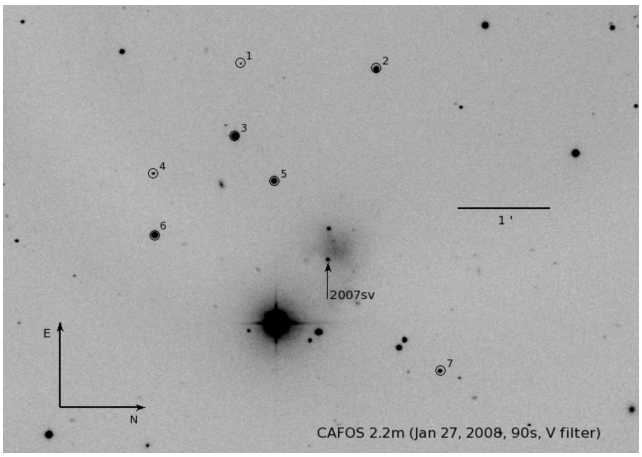

Figure 1. Finding chart of 2007sv. The stars used for the photometric calibration are labelled with a number, the position of the transient is marked with an arrow. Information about the instrumental set-up is also reported.

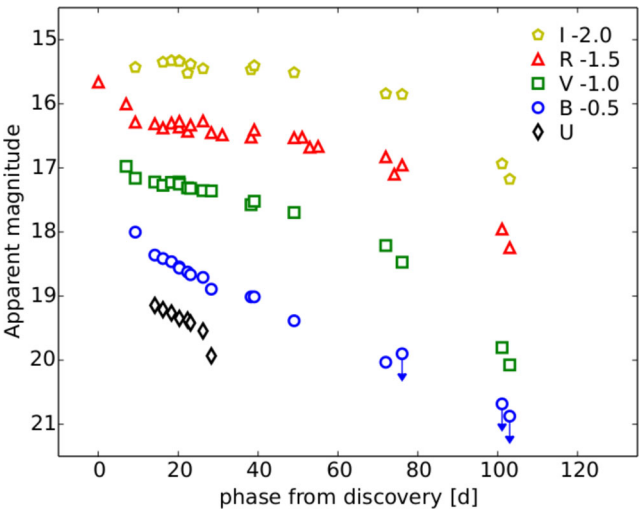

Figure 2. Multiband light curves of 2007sv. The *UBVRI* magnitudes are listed in Table 1. The phases refer to the discovery.

proximity of the maximum light. In other words, hereafter we will adopt as indicative epoch for the light-curve maximum the discovery time (2007 December 20; JD = 245 4455.41). The goodness of our assumption is supported by the photometric and spectroscopic analysis that will be widely discussed in the next sections.

Briefly, our choice is motivated on the basis of the following line of thinking. As we will discuss in the forthcoming sections, 2007sv shows very fast temperature/colour evolutions during the first 3–4

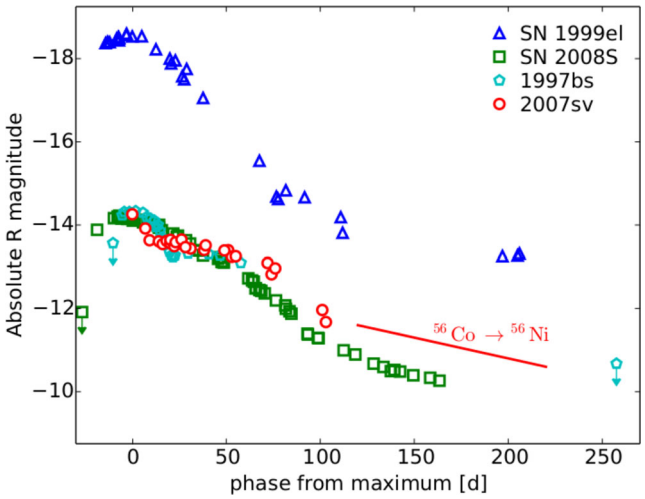

Figure 3. Comparison of the absolute *R*-band light curves of the impostors 2007sv and 1997bs, the enigmatic transient SN 2008S, and the classical Type IIn SN 1999el. The red line indicates the slope of the ^{56}Co decay.

weeks, suggesting that the transient was discovered very young, a few days after the burst. This also implies that it is unlikely that 2007sv reached a peak magnitude much brighter than the discovery magnitude $R = 17.16$ (Table 1). If we adopt for 2007sv the distance modulus and the reddening value discussed in Section 2, we obtain an absolute magnitude $M_R = -14.25 \pm 0.38$ at discovery, which is an indicative estimate for the absolute peak magnitude. This weak absolute magnitude at maximum is an indication that 2007sv was very likely an SN impostor rather than a genuine SN explosion.

3.3 Absolute magnitude and colour curves

In Fig. 3, we compare the absolute R-curve of 2007sv with those of the SN impostor 1997bs (Van Dyk et al. 2000), SN 2008S (Botticella et al. 2009) and the Type IIn SN 1999el (Di Carlo et al. 2002). As highlighted in this comparison, the absolute peak magnitude of 2007sv is similar to those measured for the SN impostor 1997bs and the enigmatic transient SN 2008S, and significantly fainter than that of a canonical SN IIn such as SN 1999el. Although the faint absolute magnitude supports the SN impostor scenario for 2007sv, this argument alone is not sufficient to rule out a true SN explosion, as we will discuss in Section 5.

The $B - V$, $V - R$ and $V - I$ colour curves of 2007sv are compared in Fig. 4 with those of the same SNe considered in Fig. 3, showing that 2007sv rapidly becomes red (in analogy with other SN impostors discovered soon after the burst) as the temperature of the ejecta rapidly decreases (Section 4). On the other hand, the regular Type IIn SN 1999el remains bluer for a longer time. In particular, it

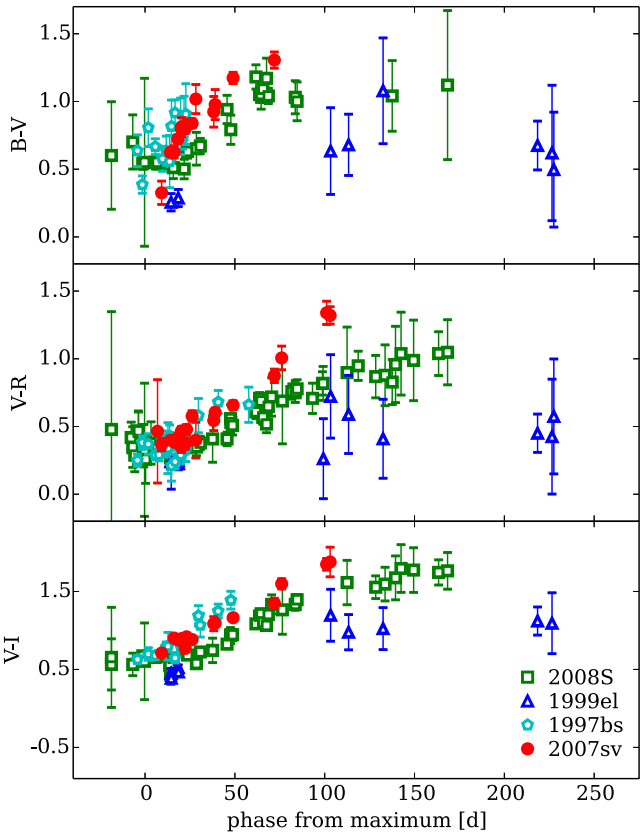

Figure 4. Comparison among the $B - V$ (top), $V - R$ (middle) and $V - I$ (bottom) colour curves of the same sample as in Fig. 3. All phases refer to the epoch of the maximum, which for 2007sv we assumed to be coincident with the discovery epoch.

has much bluer colours than the other transients at phases later than 100 d.

The comparisons shown above highlight some of the similarities between the SN impostors 2007sv and 1997bs and the peculiar transient SN 2008S, whose nature has not been firmly established yet (genuine electron-capture SN or SN impostor; see Prieto et al. 2008; Botticella et al. 2009; Pumo et al. 2009; Smith et al. 2009; Thompson et al. 2009; Wesson et al. 2010; Kochanek 2011; Szczygiel et al. 2012, and Section 4.3), all showing a fainter maximum and a different evolution in the light curve when compared with the light curve of the interacting SN 1999el.

4 SPECTROSCOPY

Spectroscopic observations were carried out from 2007 December 29 (i.e. 9 d after the discovery) to 2008 March 7 (+78 d from discovery). Basic information on the spectra and the instrumental configurations is reported in the log of spectroscopic observations (Table 3).

All data were processed using standard IRAF tasks in order to perform the pre-reduction analysis (bias, flat and overscan corrections) and the extractions of the mono-dimensional spectra. Wavelength calibration was performed using the spectra of comparison lamps obtained with the same instrumental set-up. Flux calibration was performed using the spectrum of standard stars. The accuracy of the wavelength calibration was verified measuring the wavelength of night sky lines (in particular [O I] at 5577.34 or 6300.30 Å), and a shift was applied in case of discrepancy. Spectral resolution was measured from the full width at half-maximum (FWHM) of night sky lines, adopting their mean value as final resolution estimate. The final spectral flux calibration was checked against multiband photometry obtained on the nearest night and, when necessary, a scaling factor was applied. Telluric corrections were applied when spectra of references stars obtained during the same nights were available. The spectral sequence obtained with the above procedures is shown in Fig. 5.

4.1 Spectral evolution and line identification

From Fig. 5, we note that all spectra of 2007sv are dominated by a prominent and narrow Hα emission line. We also remark that there is relatively little evolution in the spectral features during the almost 80-d coverage window, except for the continuum becoming progressively redder. As the spectra are characterized by a significant continuum contribution to the total flux, we estimated the temperature of the emitting region through a blackbody fit. The temperature experienced a rapid decline from $\simeq$8000 K in the +9 d spectrum to $\simeq$5000 K at phase $\sim$20 d. Thereafter the temperature slowly declines to $\simeq$4000 K in the late-time spectra (71–78 d; Fig. 5, see also Section 4.2). This evolution is consistent with that of the broad-band colours (Fig. 4). As mentioned above, there is little spectral evolution during the almost 80 d of spectral coverage. However, it

Table 3. Log of the spectroscopical observations of 2007sv. The phase refers to the discovery.

Date	MJD	Phase (d)	Instrumental set-up	Grism or grating	Spectral range (Å)	Resolution (Å)	Exp. times (s)
20071229	54463.96	9	Ekar182+AFOSC	2×gm4	3450–7800	24	2×1800
20080105	54470.05	15	TNG+LRS	LR-B	3600–7770	19.9	2700
20080110	54475.08	20	Ekar182+AFOSC	gm2+gm4	3450–8100	34; 24	2×1800
20080113	54478.26	23	TNG+LRS	LR-R	5070–10100	10.7	1800
20080114	54479.12	24	NOT+ALFOSC	gm4	3300–9100	9.6	1800
20080119	54484.43	30	HET	LRS	4300–7300	6.2	2×1350
20080128	54493.17	38	CAHA+CAFOS	b200	3200–8800	12.3	3600
20080201	54497.12	42	WHT+ISIS	spec	3200–10300	4.8; 9.8	1200
20080301	54526.25	71	HET	LRS	4300–7300	6.0	4×1125
20080308	54533.04	78	CAHA+CAFOS	b200+g200	4800–10700	13.8	2×2400

Notes. The spectra were obtained using the 1.82 m Telescopio Copernico with AFOSC, the 3.58 m Telescopio Nazionale Galileo (TNG) with DOLoRes (La Palma, Canary Islands, Spain), the 4.2 m William Herschel Telescope with ISIS (La Palma, Canary Islands, Spain), the 2.56 m NOT with ALFOSC, the Calar Alto 2.2 m telescope with CAFOS and the 11.1×9.8 m Hobby–Eberly Telescope (HET, Mt Fowlkes, TX, USA) with LRS.

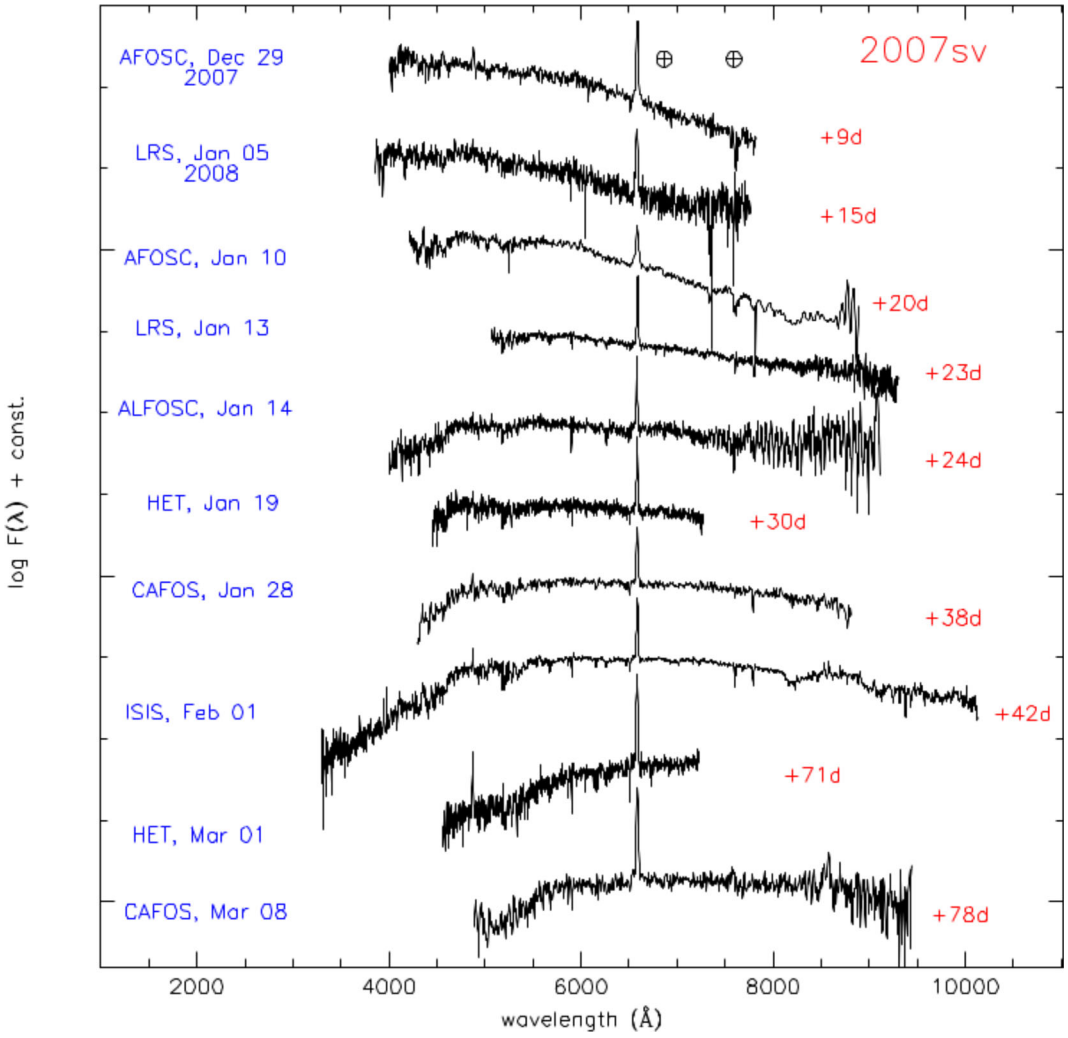

Figure 5. Spectral sequence of 2007sv. The date and the instrumental set-up are reported on the left, the phase (in days after the discovery) is indicated on the right. Spectra are flux-calibrated. The ⊕ symbols mark the position of the visible telluric absorptions.

should be noticed that the spectra have relatively poor resolution and low S/N. Therefore, it is difficult to measure evolution in the weak and narrow spectral features. In order to investigate the presence of low-contrast spectral lines, we inspected in detail one of our highest S/N spectrum (ISIS, phase +42 d).

The line identification is shown in Fig. 6. The identification was performed by comparing the spectra of 2007sv with that of the SN impostor UGC2773-20009OT1 from the Padova-Asiago SN archive (also shown in Figs 6 and 9, resolution 11 Å). A comprehensive line identification for UGC2773-2009OT1 was performed by Smith et al. (2010) and Foley et al. (2011). Fig. 6 shows that, despite the different resolution, the spectra of the two transients are very similar, with a number of lines in common (see e.g. figs 8–12 in Smith et al. 2010). We determined an indicative photospheric velocity in the spectrum of 2007sv ($\simeq$500 km s^{-1}) from the blueshifted absorption component of the Ba II 6496.6 Å line, and the expected positions of all other absorption lines were derived by adopting this velocity for all ions. The lines with strong emission components (e.g. Hα, Hβ, H&K Ca II and the NIR Ca II triplet) were identified using their rest wavelengths. We marked only multiplets with an intensity of the strongest line 5σ above the noise level. We also identified O I (multiplets 1 and 4), Ba II (multiplets 1 and 2), Na ID (doublet at 5889.9 and 5895.9 Å), Sc II (multiplets 13, 28, 29, 31), Fe II (multiplets 27, 28, 37, 38, 40, 42, 46, 48, 49, 74, 199, 200). These lines show a narrow P Cygni profile (blueshifted by about 650 km s^{-1}), although a shallow high-velocity component in the NIR Ca II triplet cannot be ruled out (see Section 4.3). We also marked the positions of the [Ca II] doublet lines at 7292 and 7324 Å, which are prominent in the spectrum of UGC2773-20009OT1 but not in the 2007sv spectrum.[6]

4.2 Hα profile and evolution of the main observables

The evolution of the Hα profile during the almost 80d of spectral coverage is highlighted in Fig. 7. We notice that there is no significant change in the wavelength position of the Hα emission peak.

The Hα line profile is relatively complex. A narrow component is detected in our higher resolution spectra of 2007sv, but a simple

[6] We also note that a telluric feature matches the wavelength position of the [Ca II] doublet, therefore no robust conclusion can be inferred on the identification of this feature in the 2007sv spectrum.

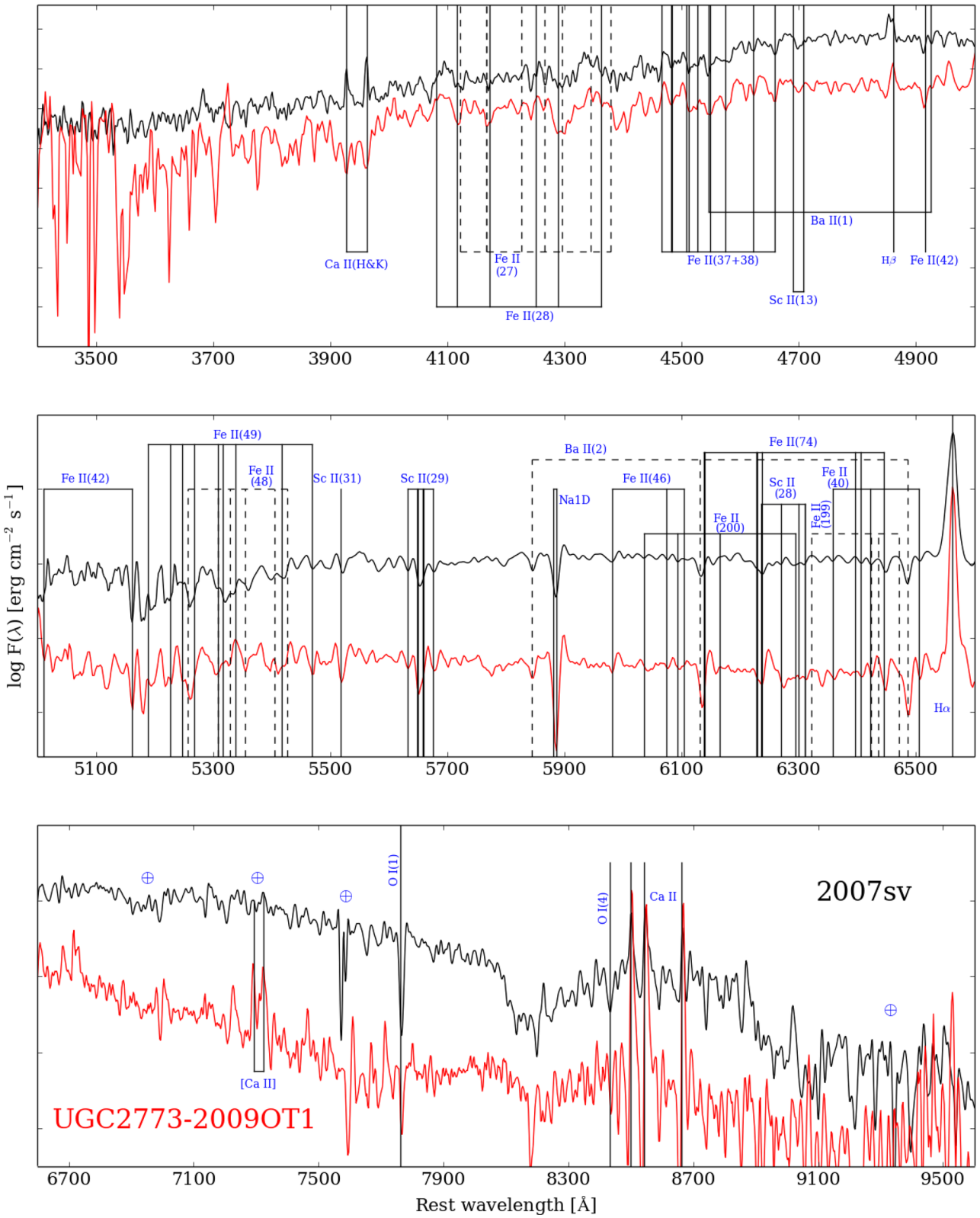

Figure 6. Line identification of the ISIS spectrum obtained on 2008 February 1 of 2007sv. A comparison with the spectrum of the transient UGC2773-2009OT1 obtained with the TNG + LRS on 2009 Oct 11 (slightly before maximum, Padova-Asiago SN archive) is also shown. The spectra are flux-calibrated and redshift-corrected. H and Ca II lines are marked at their rest wavelengths; the marks for the other lines are blueshifted by $\simeq$500 km s^{-1}. The $\oplus$ symbols mark the positions of prominent telluric absorption bands.

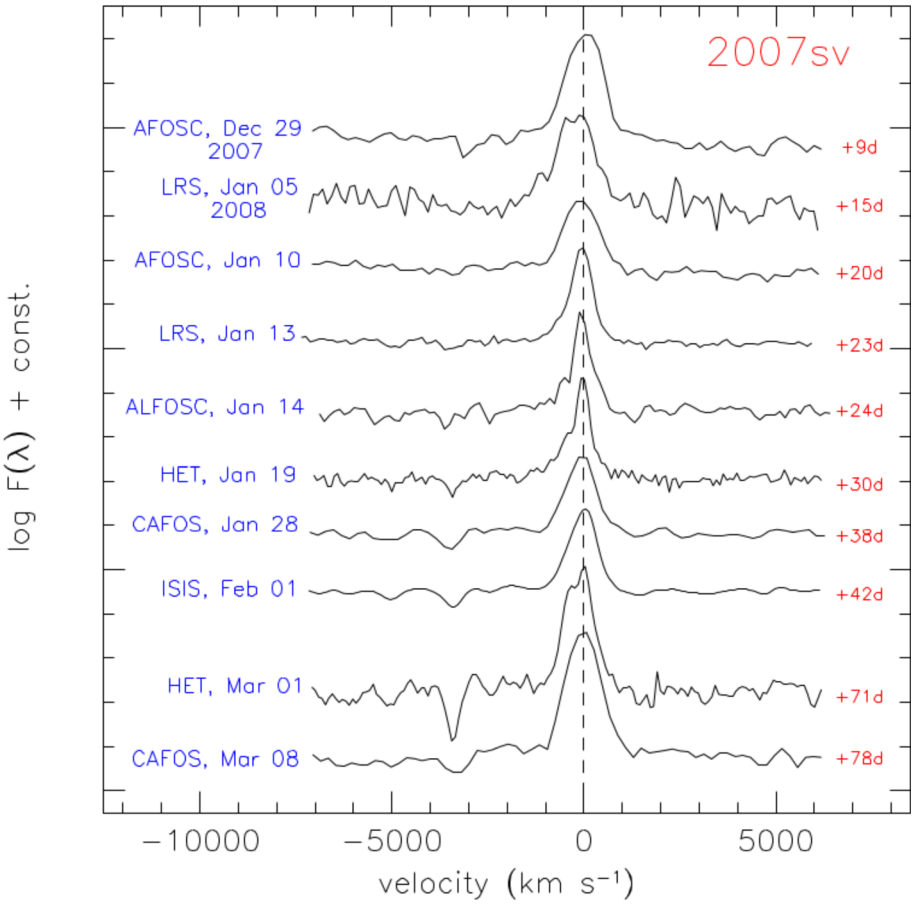

Figure 7. Evolution of the profile of Hα in the velocity space.

Gaussian or Lorentzian line fit does not well reproduce the entire line profile. For this reason, we adopted a combination of multiple line components to improve the accuracy of the spectral line fit. A broad component (decreasing from $\geq$2000 to $\simeq$1700 km s^{-1}) is visible in the two earliest spectra (phases +9 and +15 d). This component is only marginally detected in the two subsequent spectra (+20 and +23 d), and disappears at later phases. In fact, the broad component is below the detection threshold in the +24 d ALFOSC spectrum. Starting from the LRS spectrum at +23 d, we improved our fits by including an intermediate width (FWHM velocity $\approx$ 600). While we cannot rule out that the intermediate component was also present at earlier phases, the modest resolution of the +9 to +20 d spectra prevents us its discrimination from the narrow component. In the spectra collected at later phases, a two-component (intermediate + narrow) fit well reproduces the observed line profile.

In order to analyse the evolution of the velocity of the different Hα components and the total line flux, we first corrected the spectra for redshift (adopting 1116 km s^{-1} as the mean heliocentric radial velocity[7]) and for foreground Galactic extinction (using the values mentioned in Section 2). Then we measured the total line flux, and the FWHM velocities of the three Hα line components. In most spectra, the narrow component was unresolved, and even the intermediate component was occasionally below (or near) the resolution limits. In these cases, a multicomponent fit using a combination of Gaussian functions provided good fits. However, in some cases (namely for the two higher resolution HET spectra), we used a Gaussian function for the intermediate component and a Lorentzian profile for the narrow component. Fig. 8 (top panel) shows the evolution of the velocity of the ejected material for the three line components.

As mentioned above, the narrow component was unresolved in most cases. When the narrow Hα was unresolved, we used the spectral resolution as an upper limit for the velocity of the slowest moving material.

When the narrow line component was resolved, we first corrected the measured FWHM for the spectral resolution (width = $\sqrt{\mathrm{FWHM}^2 - \mathrm{res}^2}$) and then computed the velocity ($v = \frac{\mathrm{width}}{6562.8} \times c$). In the highest resolution HET (Hobby–Eberly Telescope) spectra at phases +30 and +71 d, we measured the FWHM of the narrower component as 120 $\pm$ 30 and 150 $\pm$ 40 km s^{-1}, respectively. The intermediate component remains at roughly constant velocity around 600–800 km s^{-1} at all epochs. Finally, the broad component is characterized by a fast decline from $\simeq$2000 km s^{-1} in our first spectrum to $\approx$1200 km s^{-1} in the +23 d spectrum. We note that these values are significantly smaller than the typical values of $\simeq$10 000 km s^{-1} measured in the ejecta of young SNe.

Multiple line components in the spectra of interacting objects are known to arise from different emitting gas shells (see e.g. Turatto et al. 1993). The very small velocities inferred for the narrow Hα in the HET spectra (120–150 km s^{-1}) are consistent with those expected in the winds of an LBV. The velocity evolution of the broad component is consistent with material violently ejected, and in particular with the velocities observed in the fastest

[7] http://leda.univ-lyon1.fr/

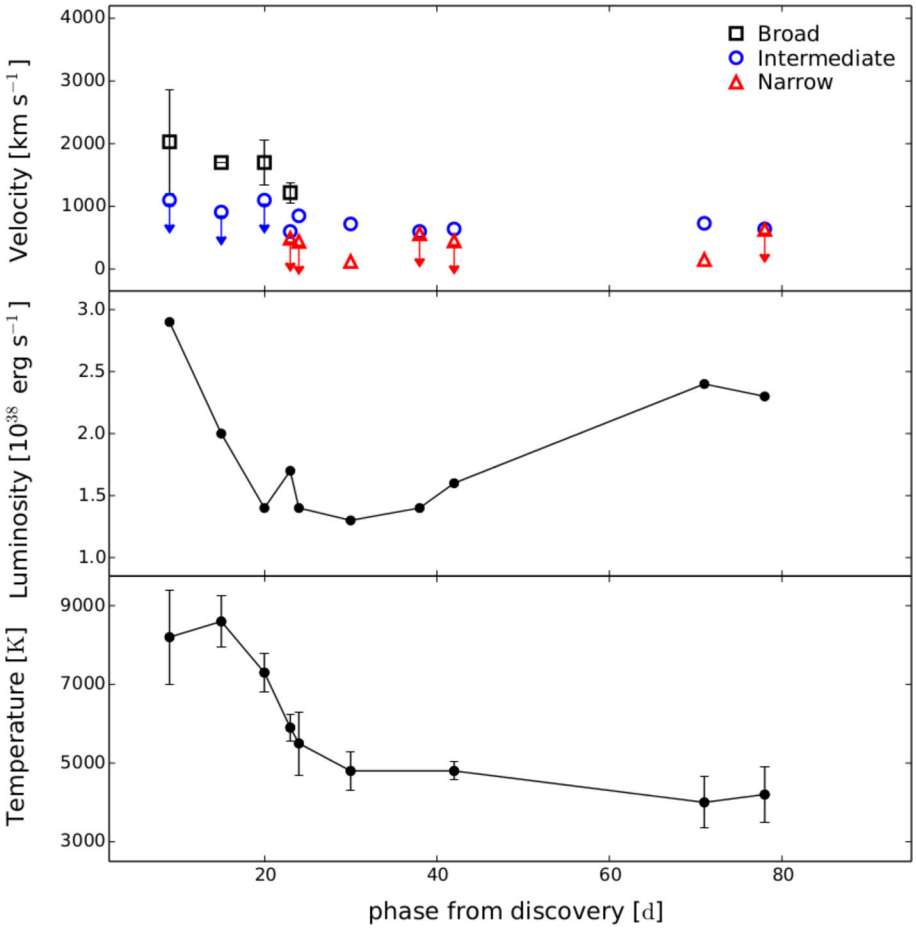

Figure 8. Top: FWHM evolution for the broad (black squares, solid line), the intermediate (blue circles) and the narrow Hα (red triangles) components. Middle: evolution of the total luminosity of Hα. We assume a 10 per cent error in the measures, due only to the error in the flux calibration. Bottom: evolution of the spectral continuum temperature.

hydrogen-rich material expelled in major eruptions of LBVs (Smith 2008; Pastorello et al. 2010, 2013). More puzzling is the interpretation of the intermediate component. According to the interpretation usually adopted in interacting SNe (see e.g. Chevalier & Fransson 1994), the intermediate velocity component arises in the gas region between the forward shock and the reverse shock. In the case of 2007sv, the relative strength of this component progressively increases with time with respect to that of the narrow component. This would support the idea that a significant fraction of the line flux at late phases arises from the gas interface between the two shock fronts, hence from the shocked gas region. In addition, one may note that the intermediate component is significantly blueshifted with respect to the narrow one. In the ejecta/circumstellar material (CSM) interaction scenario, a blueshifted intermediate component may be explained with an attenuation of the red line wind due to prompt dust formation in a post-shock cool dense shell, as observed in a number of interacting SNe (e.g. 2006jc, Mattila et al. 2008; Nozawa et al. 2008; Smith, Foley & Filippenko 2008). Alternatively, very asymmetric and blueshifted line profiles may be interpreted in terms of a highly asymmetric geometrical distribution of the CSM (see e.g. the interpretation of Stritzinger et al. 2012, for SN 2006jd).

A progressive enhancement of ejecta/CSM interaction emission can be inferred observing the evolution of the total Hα flux in the latest spectra (phase >70 d; Table 4 and Fig. 8, middle panel). The flux decreases from about 7×10^{-15} to 3×10^{-15} erg s^{-1} during the first ∼40 d. Later on, we note an increase by a factor almost two in the Hα flux, approximatively about 5.5×10^{-15} erg s^{-1} in the last two spectra. As mentioned above, this can be interpreted as an increased contribution of the intermediate component arising in a shocked gas region which dominates the flux contribution at late phases over the other line components.

4.3 Spectral comparison with other interacting transients

An important issue is to determine whether the spectroscopy alone allows us to discriminate between genuine Type IIn SNe and SN impostors. For this goal, we compare in Fig. 9 the AFOSC early-time spectrum (phase +9 d) of 2007sv with spectra of young transients with narrow emissions, viz. the impostors 1997bs (Van Dyk et al. 2000) and UGC2773-2009OT1 (Padova–Asiago SN Archive; Pastorello et al., in preparation), the classical Type IIn SN 1999el (Di Carlo et al. 2002) and SN 2008S (Botticella et al. 2009). SN 2008S is the prototype of a small family of intermediate-luminosity transients (see Thompson et al. 2009, and references therein) whose nature has been widely debated. Although many observables of SN 2008S are similar to those observed in SN impostors, the detection of prominent, narrow [Ca II] (7292–7324 Å) lines and, even more, the late-time light curve with a decline rate consistent with that expected from the ^{56}Co decay (Botticella et al. 2009), provide reasonable arguments to support a faint SN scenario. The progenitor

Table 4. Main parameters inferred from the spectra of 2007sv.

Phase (d)	FWHM($H_{\alpha,broad}$) (km s^{-1})	FWHM($H_{\alpha,intermediate}$) (km s^{-1})	FWHM($H_{\alpha,narrow}$) (km s^{-1})	H_α luminosity (10^{38} erg s^{-1})	Resolution (km s^{-1})
9	2030 ± 830	<1100	–	2.9	1100
15	1700:	<910	–	2.0	910
20	1700 ± 360	<1100	–	1.4	1100
23	1220 ± 160	600 ± 100	<490	1.7	490
24	–	850 ± 180	<440	1.4	440
30	–	720 ± 100	120 ± 30	1.3	280
38	–	600 ± 120	<560	1.4	560
42	–	640 ± 100	<450	1.6	450
71	–	730 ± 100	150 ± 40	2.4	270
78	–	640 ± 130	< 630	2.3	630

Notes. The measured FWHM of the broad, intermediate and narrow components of Hα are reported in columns 2, 3 and 4, respectively. The measure marked with the : symbol is uncertain.
The total luminosity of Hα is in column 5, the spectral resolution in column 6.

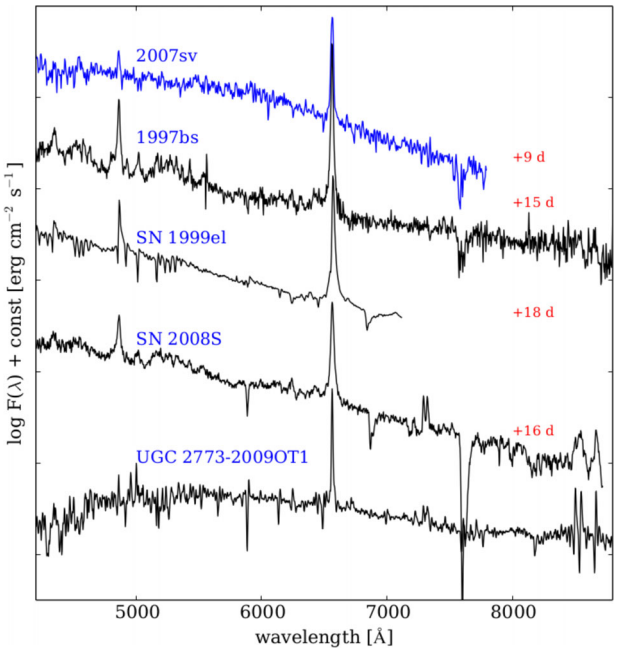

Figure 9. Comparison of early-time spectra of the impostors 2007sv, 1997bs (unpublished spectrum from the Padova–Asiago SN archive obtained on 1997 April 30 with the ESO1.52 m telescope, resolution 10 Å, located at La Silla, Chile) and UGC2773-2009OT1 (spectrum obtained slightly before maximum), the enigmatic transient SN 2008S, and the linearly declining Type IIn SN 1999el. The spectra are flux-calibrated and redshift-corrected.

star of SN 2008S was detected in mid-infrared archive *Spitzer* images, whilst there was no detection in deep optical and near-IR pre-explosion frames (e.g. Prieto et al. 2008). This was interpreted as a clear signature that the progenitor was a highly reddened star, embedded in a dusty environment. Although there is general agreement that the progenitor star of SN 2008S was a moderate-mass star,[8] the characterization of the stellar type is somewhat different in the different papers, ranging from an ∼9 $M_\odot$ extreme asymptotic giant branch star (AGB; e.g. Prieto et al. 2008; Khan et al. 2010; Kochanek 2011; Szczygiel et al. 2012) to a ≤20 $M_\odot$ supergiant (Smith et al. 2009). The most debated issue is whether the observed 2008 outburst was a terminal stellar explosion, most likely as an electron-capture (EC) SN from a super-AGB star (Pumo et al. 2009; Tominaga, Blinnikov & Nomoto 2013) or an LBV-like outburst of a mildly massive star (Smith et al. 2009, 2011).

From the comparison in Fig. 9, it is evident that the spectra of all these transients are rather similar, and many spectral lines are in common to all of them. Therefore, this is an indication that the spectra alone may not be sufficient to discriminate between impostors and true SNe. As mentioned before, the narrow [Ca II] doublet at 7292–7324 Å is the hallmark feature for SN 2008S-like transients and is sometimes used as an argument to support the SN nature of these objects. We note that there is no clear evidence for the presence of [Ca II] lines in the spectra of 2007sv or 1997bs. However, we have to admit that the [Ca II] feature was detected in UGC2773-2009OT1 (which is clearly an impostor, see Smith et al. 2010; Foley et al. 2011). Therefore, the [Ca II] feature is not a good discriminant of the nature of these explosions.

In Fig. 10, the 7800–8700 Å wavelength window of the +42 d ISIS spectrum of 2007sv is compared with spectra of SN 2008S and UGC2773-2009OT1. In all of them, we find the Ca II triplet at 8498.0, 8542.1 and 8662.1 Å, which is another very common feature in many types of transients, although some differences in the line strengths and velocities can be appreciated. The three spectra show narrow features with velocities of a few hundred km s^{-1}, and these mark the presence of slow-moving material. However, a very broad depression with a minimum at about 8200 Å is visible in all spectra in Fig. 10, suggesting that a small amount of material can be ejected at high velocities (above 10 000 km s^{-1}) also in SN impostors. The presence of fast-moving material has been also reported in the η Car circumstellar environment (Smith 2008). Therefore, the detection of high-velocity gas alone should not be considered a robust argument to favour an SN scenario.[9]

5 DISCUSSION

In Sections 3 and 4, the photometric and spectroscopic properties of the optical transient 2007sv have been described. The main goal of the forthcoming discussion is to provide convincing insights on its

[8] A similar conclusion was also inferred for the detected progenitor of the 2008S-analogous NGC300-2008OT1 (Berger, Soderberg & Chevalier 2009; Bond et al. 2009).

[9] We note, however, that this argument is instead used by many authors to favour the SN explosion scenario for the debated SN 2009ip.

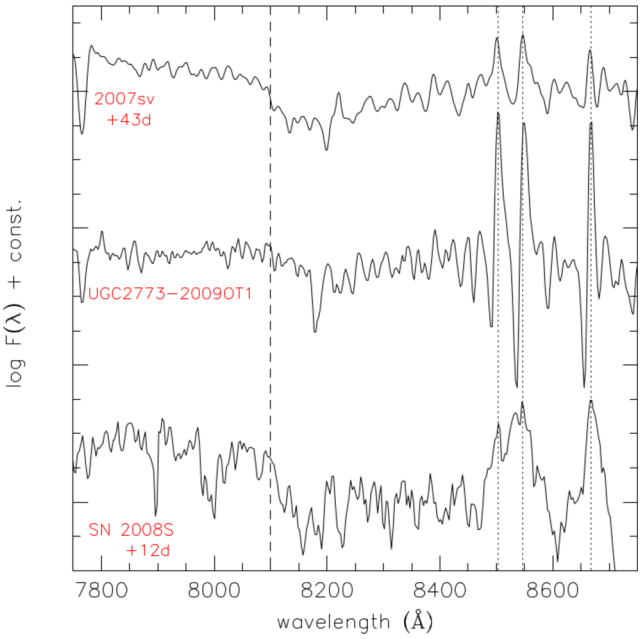

Figure 10. Comparison of the NIR Ca II triplet line profiles in three different types of faint transients, viz. 2007sv, UGC2773-2009OT1 and SN 2008S (from top to bottom). The three dotted lines mark the position of the lines of the Ca II triplet at 8498.0, 8542.1 and 8662.1 Å. The dashed is an indicative line that marks the velocity close to the terminal velocity of the gas. The spectra are flux-calibrated and redshift-corrected.

nature (SN versus SN impostor). Already from a quick investigation of the spectra of 2007sv, the similarity with the spectra of well-known SN impostors (e.g. 1997bs and UGC2773-2009OT1; Van Dyk et al. 2000; Smith et al. 2010; Foley et al. 2011) is evident. However, some similarity can also be found with the spectra of genuine interacting SNe (such as SNe 1999el and 1995G; Di Carlo et al. 2002; Pastorello et al. 2002). The comparisons shown in Section 4.3 confirm that there are only subtle differences between spectra of LBV-like eruptions and genuine Type IIn SNe, giving evidence that from the spectroscopic analysis alone it is sometimes tricky to discriminate between the two types of transients.

However, from an in-depth inspection of our spectral sequence of 2007sv, we can obtain crucial information on this object. The increased total luminosity of Hα and the enhanced strength of the intermediate-velocity component in the late-time spectra suggest that the material ejected in the outburst was interacting with the pre-existing CSM. We also found that next to the expected narrow components, Hα and the Ca II NIR triplet show broader wings (Fig. 10), suggesting an outflow of material at velocities comparable with those observed in SN ejecta. The maximum velocity registered for the outflowing material (dashed line in Fig. 10) is about 14 000 km s^{-1} (although it is clear that the bulk of this material is expanding at much lower velocity, viz. $\sim$8000 km s^{-1}). The detection of prominent broad spectral features from typical nucleosynthesis products observed in SN ejecta would be a more robust tool to distinguish between SNe and impostors. We do not detect any broad line of α- or Fe-peak elements in the late-time spectra (approx. +80 d) of 2007sv, except for the shallow absorption attributed to the Ca II NIR triplet. For this reason, the general spectral properties of 2007sv favour a non-terminal explosion scenario for this transient, although we have to admit that these cannot be considered as conclusive proofs to unveil the nature of this interacting transient.

A more robust constraint can be derived from the photometric analysis. In some cases, impostors were unmasked through their erratic light curves. It is worth mentioning the optical transient observed during the period 2000–2009 in NGC 3432 (aka 2000ch; Wagner et al. 2004; Pastorello et al. 2010) and also the 2009–2012 recurrent transient observed in NGC 7259 (known as 2009ip; Smith et al. 2010; Foley et al. 2011; Pastorello et al. 2013). The latter was followed by a major eruption in mid-2012 that has been proposed to be a terminal SN explosion (Smith et al. 2014, and references therein). However, more frequently impostors reveal themselves through a single episode, characterized by a fast-evolving but regular light curve. A classical example is 1997bs (Van Dyk et al. 2000), whose light-curve shape is not trivially discernible from that of a regular SN. And the light curve of 2007sv is remarkably similar to that of 1997bs. However, the colours of 2007sv rapidly become redder as the object evolves, due to the decreasing temperature of the emitting region (this finding is confirmed by the temperature evolution inferred through blackbody fits to the spectral continuum). The colour/temperature transition is observed to occur on much shorter time-scales than in typical SNe IIn (see e.g. Fig. 4).

Finally, the peak luminosity still remains the most used method to discriminate between SNe and impostors. With a distance modulus of 31.38 ± 0.27 mag, we derive for 2007sv an absolute magnitude of $M_R = -14.25 \pm 0.38$. This value is 4–6 mag fainter than the absolute magnitudes typically measured in Type IIn SNe (e.g. Richardson et al. 2002).

5.1 Which mechanisms can produce 2007sv-like events?

The faint absolute magnitude at the discovery and the rapid colour (temperature) evolution provide robust evidence for the impostor nature for 2007sv, though some cases of faint transients exist in the literature that have been proposed to be true SNe. In fact, weak SNe can be produced* via (i) the core-collapse explosion of a peculiar SN through EC of a moderate-mass star; (ii) the fall back event from a very massive star (Pumo et al. 2009, and references therein). Both mechanisms are believed to produce absolute light curves fainter than those observed in canonical SN types.

In the former scenario, the ONeMg stellar core of an 8–10 $M_\odot$ super-AGB star collapses generating a weak, low-energy event called EC SN. The SN ejecta may eventually interact with an H-rich circumstellar environment generated by the stellar mass-loss during the super-AGB phase. As mentioned in Section 4.3, a promising candidate EC SN is SN 2008S (Botticella et al. 2009), an object that shares some similarity with an SN impostor, but has an SN-like shaped light curve, a late-time light curve consistent with the ^{56}Co decay. In the latter scenario, the collapse of a very massive star ($>$25–30 $M_\odot$; Zampieri et al. 2003) is followed by the fall-back of the inner stellar mantle on to the stellar core, generating eventually a black hole. In both scenarios a common feature is the faint absolute magnitude, which is generally due to the small amount of radioactive ^{56}Ni in the ejecta. The presence of radioactive material in the ejecta can be revealed from the decline rate of the late-time SN light curve. However, in massive stars the interaction of the ejecta with the pre-existing CSM can induce a dramatic increase in the radiated energy, and cause significant deviations from the expected luminosity peak and light-curve decline rate expected in the radioactive decays, making the detection of ^{56}Co signatures problematic.

Another efficient mechanism proposed to explain transient events with a total radiated energy comparable with those of real SNe

is the pulsational pair-instability in very massive stars. Woosley, Blinnikov & Heger (2007) showed that major instabilities produced by electron–positron pair production (pulsational-pair instability) cause the ejection of massive shells without necessarily unbinding the star (and hence without leading to a terminal SN explosion). These major mass-loss episodes might produce transients currently classified as SN impostors. In addition to this, when a new shell is ejected and collides with pre-existing material, the resulting radiated energy is comparable with that of a core-collapse SN (CC-SN, sometimes even one order of magnitude higher). If the impacting material is H-rich, the shell–shell collisions would produce an SN IIn-like spectrum and a slowly evolving, luminous light curve that would make the transient practically indiscernible from true SNe IIn. All of this further complicates our attempts of discriminating SNe IIn from eruptive impostors.

A safe discrimination criterion would be the detection of the products of stellar and core-collapse explosive nucleosynthesis through the prominent α-element lines in the nebular spectra. But in many SNe IIn the inner ejecta are covered by the H-rich interaction region sometimes for very long time-scales (up to many years), making the detection of the α-element spectral features difficult.

All the clues illustrated so far make us confident that 2007sv was not a terminal SN explosion, but very likely a major eruption mimicking the SN behaviour. If this is true, the progenitor star may have reached again a quiescent stage, returning to the pre-eruptive bolometric luminosity. This can be confirmed through an inspection of deep, high-resolution images obtained years after the outburst, for example using the *Hubble Space Telescope* (*HST*) or the largest ground based telescopes which can deliver sub-arcsecond images. The identification of the quiescent progenitor in such high-quality images would be final evidence that the massive star producing 2007sv is still alive. Alternatively, a long time-scale monitoring of 2007sv can eventually reveal further outbursts after the one registered in 2007, which would also prove that the 2007 episode was not the final stellar death. This strategy worked well for the 2000 transient observed in NGC 3432 (Wagner et al. 2004) that was recovered after 8 yr during a subsequent eruptive phase (Pastorello et al. 2010).

5.2 Is 2007sv heralding an SN explosion?

In order to identity possible further outbursts experienced by the progenitor of 2007sv, we analysed a number of images of the transient site obtained before and after the 2007 event. These data were mostly collected by two of the co-authors of this paper (TB and GB), with a few additional observations performed with the 1.82 m Telescopio Copernico of the Asiago Observatory. These observations are listed in Table A1 in Appendix A. The unfiltered observations of TB and GB were scaled to *R*-band magnitudes using the magnitudes of references stars reported in Table 2. These images of the 2007sv site span a period of over a decade. In this temporal window, we did not detect any further signature of a variable source at the position of 2007sv (see Fig. 11). The Pan-STARRS1 survey (PS1) imaged this galaxy on 52 separate nights between 2010 February 25 (MJD 55252.30) and 2013 May 17 (MJD 56429.26) in one of the filters $g_{\rm P1}r_{\rm P1}i_{\rm P1}z_{\rm P1}$ (for a description of the Pan-STARRS1 3π survey; see Inserra et al. 2013; Magnier et al. 2013). No further detection of any outbursting activity was seen, and the magnitude limits of these individual epochs are typically 22.0, 21.6, 21.7, 21.4 and 19.3, respectively, for $g_{\rm P1}r_{\rm P1}i_{\rm P1}z_{\rm P1}$ (as reported in Inserra et al. 2013). These magnitudes are in the AB system as reported in Tonry et al. (2012).

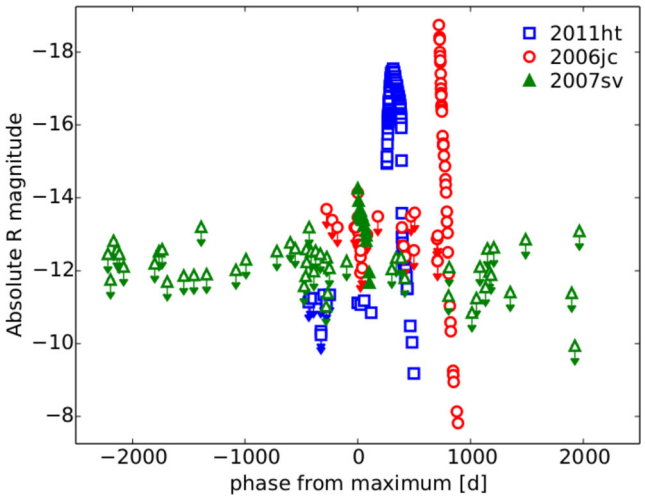

Figure 11. Plot of the photometric limits obtained from 2001 November 27 to 2014 January 07 and the absolute *R*-band light curve of 2007sv. The absolute light curve of the Type Ibn SN 2006jc and the Type IIn SN 2011ht are shown for comparison. The phases refer to the first recorded eruption.

Tracing the photometric history of an SN impostor has also another objective. As briefly mentioned in Section 1, there is growing evidence that some interacting SNe may be preceded by large stellar eruptions (i.e. impostor events). A similar sequence of events has been proposed for a number of SNe, from the historical case of SN 2006jc discovered by K. Itagaki (Nakano et al. 2006; Yamaoka, Nakano & Itagaki 2006; Pastorello et al. 2007) to a few recent Type IIn SNe (see Smith et al. 2014, and references therein). In several cases, a lower luminosity outburst was observed few weeks before the brightest event (i.e. the putative SN). However, occasionally a larger time delay was observed between the two episodes (1–2 yr). In Fig. 11, together with 2007sv, we also show two cases of SNe that were heralded by an outburst with a significant time delay. SN 2006jc is a stripped-envelope SN (of type Ibn) whose ejecta were seen to interact with He-rich CSM (Foley et al. 2007; Pastorello et al. 2007, 2008). Its progenitor experienced an outburst 2 yr before its explosion as a CC-SN, and the magnitude of this impostor ($M_R \simeq -14$) was comparable with that expected in an LBV eruption. SN 2011ht was initially classified as an SN impostor on the basis of its early spectral properties (Pastorello et al. 2011), and was later reclassified as a Type IIn SN after a major spectral metamorphosis (Prieto et al. 2011). However, the nature of SN 2011ht nature is not fully clarified. There are controversial interpretations on its SN-like observables (Humphreys et al. 2012; Roming, Pritchard & Prieto 2012; Fraser et al. 2013; Mauerhan et al. 2013), since collisions among massive shells might still explain SN 2011ht without necessarily invoking a core-collapse. Interestingly, a posteriori, a weak transient has been observed about one year before the main episode (Fraser et al. 2013). This weak source, (labelled as PSO J152.0441+51.8492 by Fraser et al. 2013) was detected in archival data of the Panoramic Survey Telescope and Rapid Response System 1 (Pan-STARRS1) at an absolute magnitude $M_R \approx -11.8$. Fraser et al. (2013) provided strong arguments that the two sources were physically related. Recent studies (see Ofek et al. 2014) claim that pre-SN eruptions are quite common. None the less, so far only an handful of impostors with solid detections have been observed to be followed by what is believed to be a true SN explosion.

The most intriguing issue is that, although there are some outliers with the absolute magnitudes brighter than −14 (Ofek et al. 2014), most pre-SN outbursts (those with robust detections) have absolute magnitudes close to or fainter than −14, nearly coincident with absolute magnitude of 2007sv. Although there was no further detection of a re-brightening of 2007sv before and after 2007, its overall photometric similarity with the precursors of SN 2006jc and other interacting SNe, may lead to the speculation that impostors such as 2007sv are instability episodes of massive stars (some of them in the LBV stage) that can be followed on short time-scales (months to decades) by a terminal stellar explosion, as an ejecta-CSM interacting SN.

6 CONCLUSIONS

In this paper, we have reported the results of our follow-up campaign of the transient 2007sv. Our photometric monitoring spans a period of over 100 d, whilst our spectroscopy data cover ≃80 d of the evolution of 2007sv. The spectra are largely dominated by a multicomponent Hα line in emission. This spectral characteristic is common to both in SN impostors and in Type IIn SNe.

As we have illustrated, though there are uncertainties on the observational constraints and the discrimination between true interacting SNe and SN impostors is often a tricky issue, the lack of broad lines from α-elements, the fast colour/temperature evolutions, together with the relatively low velocity of the ejecta and the faint absolute magnitude at discovery ($M_R = -14.25$) support the SN impostor scenario for 2007sv, most likely a major eruption of an LBV. Although we do not have stringent pre-discovery limits, we claim that 2007sv was discovered soon after the outburst. Hence, we have adopted the discovery magnitude as an indicative guess for the peak magnitude. This is supported by the rapid evolution of the colours and the temperature of the ejecta in the early phases supports this assumption.

However, some doubts still remain whether 2007sv was instead a very weak terminal explosion of a massive star. In absence of the detection of further outbursts or a future 'real' SN explosion (as observed in other similar transients), the most promising method to definitely rule out the possibility that 2007sv was a faint interacting CC-SN is by obtaining deep and high spatial resolution images of the transient's site (e.g. with *HST*), in the attempt to detect some signatures from the surviving star. This method, that has been successfully tested to find the progenitors of a number of CC-SNe (see Smartt 2009, and references therein) and may well give the final answer to the enigma of 2007sv.

ACKNOWLEDGEMENTS

This research has made use of the NASA/IPAC Extragalactic Database (NED) which is operated by the Jet Propulsion Laboratory, California Institute of Technology, under contract with the National Aeronautics and Space Administration.

We acknowledge the usage of the HyperLeda database (http://leda.univ-lyon1.fr).

Based on observations made with:

(i) The Cima Ekar 1.82 m telescope of the INAF-Astronomical Observatory of Padua, Italy.

(ii) The Liverpool Telescope operated on the island of La Palma by Liverpool John Moores University in the Spanish Observatorio del Roque de los Muchachos of the Instituto de Astrofisica de Canarias with financial support from the UK Science and Technology Facilities Council.

(iii) The Nordic Optical Telescope (NOT), operated by the NOT Scientific Association at the Observatorio del Roque de los Muchachos, La Palma, Spain, of the Instituto de Astrofisica de Canarias.

(iv) The William Herschel Telescope (WHT) operated on the island of La Palma by the Isaac Newton Group in the Spanish Observatorio del Roque de los Muchachos of the Instituto de Astrofsica de Canarias.

(v) The Italian Telescopio Nazionale Galileo (TNG) operated on the island of La Palma by the Fundacion Galileo Galilei of the INAF (Istituto Nazionale di Astrofisica) at the Spanish Observatorio del Roque de los Muchachos of the Instituto de Astrofisica de Canarias.

(vi) The Hobby-Eberly Telescope (HET), joint project of the University of Texas at Austin, Pennsylvania State University, Stanford University, Ludwig-Maximilians-Universität München, and Georg-August-Universität Göttingen.

(vii) The Calar Alto 2.2 m telescope operated at the Centro Astronomico Hispano Aleman (CAHA) at Calar Alto, owned and operated jointly by the Max-Planck-Institut für Astronomie in Heidelberg, Germany, and the Instituto de Astrofisica de Andalucia in Granada, Spain.

We thank P. Corelli (Mandi observatory, Pagnacco, UD, Italy) for the observations of (SN) 2007sv.

Based also on observations performed at the NOT (Proposal number 49-016, PI: F. Taddia), La Palma, Spain.

This work is part of the European supernova collaboration involved in the ESO-NTT large programme 184.D-1140 led by Stefano Benetti.

LT, AP, SB, EC, AH and MT are partially supported by the PRIN-INAF 2011 with the project 'Transient Universe: from ESO Large to PESSTO'.

NER is supported by the MICINN grant AYA2011-24704/ESP, by the ESF EUROCORES Program EuroGENESIS (MICINN grant EUI2009-04170), by SGR grants of the Generalitat de Catalunya, and by EU-FEDER funds.

NER also acknowledges the support from the European Union Seventh Framework Programme (FP7/2007-2013) under grant agreement no. 267251.

ST acknowledges support by TRR 33 'The Dark Universe' of the German Research Foundation (DFG).

The research of JRM is supported through a Royal Society Research Fellowship.

The research leading to these results has received funding from the European Research Council under the European Union's Seventh Framework Programme (FP7/2007-2013)/ERC Grant agreement no. [291222] (PI: S. J. Smartt).

FB acknowledges support from FONDECYT through Postdoctoral grant 3120227 and from Project IC120009 'Millennium Institute of Astrophysics (MAS)' of the Iniciativa Científica Milenio del Ministerio de Economía, Fomento y Turismo de Chile.

The PS1 have been made possible through contributions of the Institute for Astronomy, the University of Hawaii, the Pan-STARRS Project Office, the Max-Planck Society and its participating institutes, the Max Planck Institute for Astronomy, Heidelberg and the Max Planck Institute for Extraterrestrial Physics, Garching, The Johns Hopkins University, Durham University, the University of Edinburgh, Queen's University Belfast, the Harvard–Smithsonian Center for Astrophysics, the Las Cumbres Observatory Global Telescope Network Incorporated, the National Central University of Taiwan, the Space Telescope Science Institute, the National

Aeronautics and Space Administration under Grant No. NNX08AR22G issued through the Planetary Science Division of the NASA Science Mission Directorate, the National Science Foundation under Grant No. AST-1238877, the University of Maryland, and Eotvos Lorand University (ELTE).

REFERENCES

Berger E., Soderberg A. M., Chevalier R. A., 2009, ApJ, 699, 1850
Bond H. E., Bedin L. R., Bonanos A. Z., Humphreys R. M., Monard L. A. G. B., Prieto J. L., Walter F. M., 2009, ApJ, 695, L154
Botticella M. T. et al., 2009, MNRAS, 398, 1041
Chevalier R. A., Fransson C., 1994, ApJ, 420, 268
Corwin H. G., de Vaucouleurs A., de Vaucouleurs G., 1985, University of Texas Monographs in Astronomy, Southern Galaxy Catalogue. A Catalogue of 5481 Galaxies South of Declination -17 grad. Found on 1.2m UK Schmidt IIIa J Plates. Univ. Texas Press, Austin, TX
Dessart L., Hillier D. J., Gezari S., Basa S., Matheson T., 2009, MNRAS, 394, 21
Di Carlo E. et al., 2002, ApJ, 573, 144
Duszanowicz G., Boles T., Corelli P., 2007, Cent. Bur. Electron. Telegrams, 1182, 1
Foley R. J., Smith N., Ganeshalingam M., Li W., Chornock R., Filippenko A. V., 2007, ApJ, 657, L105
Foley R. J., Berger E., Fox O., Levesque E. M., Challis P. J., Ivans I. I., Rhoads J. E., Soderberg A. M., 2011, ApJ, 732, 32
Fraser M. et al., 2013, ApJ, 779, L8
Gal-Yam A., Leonard D. C., 2009, Nature, 458, 865
Grebel E. K., 2001, Ap&SS, 277, 231
Habergham S. M., Anderson J. P., James P. A., Lyman J. D., 2014, MNRAS, 441, 2230
Humphreys R. M., Davidson K., 1994, PASP, 106, 1025
Humphreys R. M., Davidson K., Jones T. J., Pogge R. W., Grammer S. H., Prieto J. L., Pritchard T. A., 2012, ApJ, 760, 93
Inserra C. et al., 2013, ApJ, 770, 128
Khan R., Stanek K. Z., Prieto J. L., Kochanek C. S., Thompson T. A., Beacom J. F., 2010, ApJ, 715, 1094
Kochanek C. S., 2011, ApJ, 741, 37
Kotak R., Vink J., 2006, A&A, 460, L5
Landolt A. U., 1992, AJ, 104, 340
Magnier E. A. et al., 2013, ApJs, 205, 20
Margutti R. et al., 2014, ApJ, 780, 21
Mattila S. et al., 2008, MNRAS, 389, 141
Mauerhan J. C. et al., 2013, MNRAS, 431, 2599
Maund J. R. et al., 2006, MNRAS, 369, 390
Nakano S., Itagaki K., Puckett T., Gorelli R., 2006, Cent. Bur. Electron. Telegrams, 666, 1
Nozawa T. et al., 2008, ApJ, 684, 1343
Ofek E. O. et al., 2013, Nature, 494, 65
Ofek E. O. et al., 2014, ApJ, 789, 104
Pastorello A. et al., 2002, MNRAS, 333, 27
Pastorello A. et al., 2007, Nature, 447, 829
Pastorello A. et al., 2008, MNRAS, 389, 113
Pastorello A., Stanishev V., Smartt S. J., Fraser M., Lindborg M., 2011, Cent. Bur. Electron. Telegrams, 2851, 2
Pastorello A. et al., 2012, MNRAS, 408, 181
Pastorello A. et al., 2013, ApJ, 767, 1
Paturel G., Petit C., Prugniel Ph., Theureau G., Rousseau J., Brouty M., Dubois P., Cambrésy L., 2003, A&A, 412, 45
Pettini M., Pagel B. E. J., 2004, MNRAS, 348, L59
Pilyugin L. S., Vílchez J. M., Contini T., 2004, A&A, 425, 849
Prieto J. L. et al., 2008, ApJ, 681, L9
Prieto J. L., McMillan R., Bakos G., Grennan D., 2011, Cent. Bur. Electron. Telegrams, 2903, 1
Pumo M. L. et al., 2009, ApJ, 705, L138
Richardson D., Branch D., Casebeer D., Millard J., Thomas R. C., Baron E., 2002, AJ, 123, 745
Roming P. W. A., Pritchard T. A., Prieto J. L., 2012, ApJ, 751, 92
Schlafly E. F., Finkbeiner D. P., 2011, ApJ, 737, 103
Schlegel D. J., Finkbeiner D. P., Davis M., 1998, ApJ, 500, 525
Smartt S. J., 2009, ARA&A, 47, 63
Smith N., 2008, Nature, 455, 201
Smith N., Foley R. J., Filippenko A. V., 2008, ApJ, 687, 1208
Smith N. et al., 2009, ApJ, 679, L49
Smith N. et al., 2010, AJ, 139, 1451
Smith N., Li W., Silverman J. M., Ganeshalingam M., Filippenko A. V., 2011, MNRAS, 415, 773
Smith N., Mauerhan J. C., Prieto J., 2014, MNRAS, 438, 1191
Stritzinger M. et al., 2012, ApJ, 756, 173
Szczygiel D. M., Prieto J. L., Kochanek C. S., Stanek K. Z., Thompson T. A., Beacom J. F., Garnavich P. M., Woodward C. E., 2012, ApJ, 750, 77
Taddia F. et al., 2013, A&A, 558, A143
Tammann G. A., 1994, in Meylan G., Prugniel P., eds, ESO Conference and Workshop Proc., 49, Dwarf Galaxies. ESO, Garching, p. 3
Thompson T. A., Prieto J. L., Stanek K. Z., Kistler M. D., Beacom J. F., Kochanek C. S., 2009, ApJ, 705, 1364
Tominaga N., Blinnikov S. I., Nomoto K., 2013, ApJ, 771, L12
Tonry J. L. et al., 2012, ApJ, 750, 99
Turatto M., Cappellaro E., Danziger I. J., Benetti S., Gouiffes C., della Valle M., 1993, MNRAS, 262, 128
van den Bergh S., 1960, ApJ, 131, 215
Van Dyk S. D., Matheson T., 2012, in, ed. Astrophysics and Space Science Library, Vol. 384. Eta Carinae and the Supernova Impostors. Springer-Verlag, Berlin, p. 249
Van Dyk S. D., Peng C. Y., King J. Y., Filippenko A. V., Treffers R. R., Li W., Richmond M. W., 2000, PASP, 112, 1532
Wagner R. M. et al., 2004, PASP, 116, 326
Wesson R. et al., 2010, MNRAS, 403, 474
Wolf B., 1989, A&A, 217, 87
Woosley S. E., Blinnikov S., Heger A., 2007, Nature, 450, 390
Yamaoka H., Nakano S., Itagaki K., 2006, Cent. Bur. Electron. Telegrams, 666, 2
Zampieri L., Pastorello A., Turatto M., Cappellaro E., Benetti S., Altavilla G., Mazzali P., Hamuy M., 2003, MNRAS, 338, 711

APPENDIX A: PHOTOMETRIC LIMITS OF 2007SV

Table A1. Optical detection limits for 2007sv. No source was observed in the position of the transient at any epochs reported in the table.

Date	MJD	*R*	Instrument
20011127	52240.11	>18.96	Apogee AP7
20011220	52263.09	>19.66	Apogee AP7
20020116	52290.20	>18.60	Apogee AP7
20020215	52320.81	>18.85	Apogee AP7
20020307	52340.86	>18.96	Apogee AP7
20020414	52378.95	>19.30	Apogee AP7
20030115	52654.91	>19.22	Apogee AP7
20030222	52692.91	>18.89	Apogee AP7
20030323	52721.03	>18.84	Apogee AP7
20030506	52765.91	>19.72	Apogee AP7
20030930	52912.17	>19.55	Apogee AP7
20031229	53002.03	>19.54	Apogee AP7
20040302	53066.83	>18.22	Apogee AP7
20040419	53114.94	>19.51	Apogee AP7
20050105	53375.00	>19.39	Apogee AP7
20050403	53463.98	>19.11	Apogee AP7
20060103	53738.05	>18.89	SX
20060305	53899.87	>18.81	Apogee AP7
20060501	53856.89	>18.65	Apogee AP7
20060831	53978.90	>19.84	SX

Table A1 – *continued*

Date	MJD	*R*	Instrument
20060915	53993.00	>19.56	SX
20060920	53998.95	>18.83	SX
20060923	54001.87	>19.18	SX
20061015	54023.78	>18.23	SX
20061103	54042.08	>18.89	SX
20061126	54065.91	>19.43	SX
20061223	54081.06	>18.88	SX
20070122	54122.88	>18.96	SX
20070314	54173.86	>20.39	SX
20070321	54180.88	>19.05	Apogee AP7
20070328	54187.84	>20.03	SX
20070413	54203.85	>19.34	SX
20070913	54356.09	>19.16	SX
20081017	54756.97	>19.37	SX
20081125	54795.98	>19.05	SX
20090107	54838.84	>19.06	SX
20090209	54871.83	>19.62	SX
20100304	55259.84	>20.10	Apogee AP7
20100310	55265.80	>19.32	SX
20100928	55467.13	>20.57	SX
20101107	55507.13	>20.17	SX
20101207	55537.95	>19.31	SX
20110126	55587.84	>19.87	SX
20110212	55604.81	>18.82	Apogee AP7
20110302	55622.86	>19.44	SX
20110316	55636.87	>19.53	SX
20110409	55660.94	>18.79	Apogee AP7
20110903	55807.07	>20.01	SX
20120117	55943.21	>18.56	Apogee AP7
20130228	56351.89	>20.03	ARTEMIS
20130315	56379.86	>21.48	ARTEMIS
20130320	56371.10	>21.88	AFOSC
20130507	56419.92	>18.34	Apogee AP7
20131205	56631.19	>22.15	AFOSC
20140107	56664.99	>21.29	AFOSC

Notes. The observations provided by TB (with a C-14 Celestron Schmidt Cassegrain reflector and an Apogee AP7 CCD camera at the Coddenham Astronomical Observatory, Suffolk, United Kingdom) and GD (with a 0.32 m f/3.1 reflector and a Starlight Xpress MX716 CCD camera at Moonbase Observatory, Akersberga, Sweden) were unfiltered images, with magnitudes rescaled to the *R* band.

Multiband observations were obtained on 2013 March 20 with the following additional detection limits: $U > 19.93$, $B > 20.94$, $V > 21.02$, $I > 21.26$.

This paper has been typeset from a TEX/LATEX file prepared by the author.